The definitive version of the text was subsequently published in: Quaternary International, 2014, Volume 319, pp. 22-37, 15 January 2014, ISSN 1040-6182.
doi:10.1016/j.quaint.2012.04.004

The Paks loess-paleosol sequence: a record of chemical weathering and provenance for the last 800 ka in the mid-Carpathian Basin

Gábor Újvári[1*], Andrea Varga[2], Béla Raucsik[2], János Kovács[2]

[1]Geodetic and Geophysical Institute, Research Centre for Astronomy and Earth Sciences, Hungarian Academy of Sciences, Csatkai E. u. 6-8, H-9400 Sopron, Hungary

[2]Department of Geology, University of Pécs, Ifjúság útja 6, H-7624 Pécs, Hungary

*Corresponding author. E-mail: ujvari@ggki.hu

Abstract

The Paks loess-paleosol sequence is one of the most important terrestrial records of Middle and Late Pleistocene environmental changes in East Central Europe, spanning the last ca. 0.8 Ma. While geochemical proxies demonstrate a general decreasing chemical weathering trend over the last 0.8 Ma in the Carpathian Basin, mineralogy and derived indices reflect intensifying physical erosion. In theory, the observed chemical weathering trend can be accounted for both by enhanced input of relatively unweathered material and by climate deterioration during the Quaternary, as the used proxies like CIA are not capable of distinguishing between pre- and post-depositional weathering. Enhanced physical erosion of the source areas, driven by tectonism, and resulting increased sedimentation of fresh mineral dust at the depositional site are demonstrated by increasing dolomite, illite and chlorite contents and sme/ill, sme/(ill+chl) ratios from older to younger sediments in the profile, together with increasing thickness of loess layers towards the youngest part of the sequence. At the same time, constant smectite contents (30-40%) in paleosols appear to disprove progressive aridization of interglacials through time and suggest that the duration of pedogenesis played an important role in determining soil types. Further, the increasing proportion of inherited phyllosilicates (illite and chlorite) would, in theory, raise the possibility that the decreasing values of chemical weathering indices are just artifacts of enhanced physical erosion and resulting increased dust deposition by a dilution effect. The above findings highlight the fact that our general view on chemical weathering is oversimplistic, as its 'equation' includes two basic variables, tectonism

and time beyond climate and the interplay of these equally important factors will eventually determine its final value. To get a better grasp of these processes one needs further data (more age control in loess profiles, data on uplift in and around sedimentary basins) and more sophisticated proxies, as the mineralogical data presented here can be considered only semi-quantitative.

Regarding the provenance of sediments in the Paks profile, geochemical data demonstrate that felsic rocks dominated the source areas and there have been only very little variations in provenance over the last ca. 0.8 Ma. Significant contributions from mafic/ultramafic rocks to the sediments can be ruled out as revealed by lower abundances of ferromagnesian trace elements. The appearance of amphiboles and high dolomite contents suggest that loess material was at least partly sourced from local rocks and geochemical data reveal a genetic link between floodplain sediments and loess deposits.

Keywords: loess-paleosol mineralogy, geochemistry, chemical weathering, tectonism, paleoclimate, Quaternary

1. Introduction

Long, continuous terrestrial archives of climate and environment are rare. Lake sequences are continuous, but they mostly provide a record of past climate history of some thousands or ten thousands of years. At the same time, loess-paleosol sequences cannot be regarded as continuous records of changing palaeoenvironments (Kemp, 2001), but they yield records on time scales of 10^5 to 10^6 years. There are only some unique loess sequences in East Central Europe such as e.g. the Krems loess profile (Fink and Kukla, 1977), the Udvari 2A borehole (Koloszár, 2010), the Koriten and Viatovo loess profiles (Jordanova and Petersen, 1999; Jordanova et al., 2007) and the recently investigated Stari Slankamen loess-paleosol sequence (Marković et al., 2011), which span the last ca. 0.8 to 1 million years. According to paleomagnetic studies, the Paks loess-paleosol sequence in Hungary also belongs to these profiles providing a Quaternary climatic record of over 0.8 Ma (Pécsi and Pevzner, 1974; Pécsi, 1979; Sartori et al., 1999).

Beyond magnetic susceptibility and grain size, bulk and clay mineralogy and bulk chemistry may provide insight into the long-term regional climatic and weathering history of the Carpathian Basin during the Middle and Late Pleistocene. As the Paks loess record contains these information on tectonic timescales the issue of tectonic, climatic and sedimentological influences on chemical weathering can also be addressed (Varga et al., 2011). Further, by using mineralogical and geochemical data additional information on provenance of loess material is expected to be gained (Muhs et al., 2008; Buggle et al., 2008; Újvári et al., 2008). With our study, performed on the Paks loess profile, we intended to improve our understanding of the above issues and complement the existing high-resolution magnetic susceptibiliy and low-resolution grain size datasets published so far. Finally, by publishing our data a regional-scale, geochemistry-based correlation framework is going to be initiated.

2. Geological settings and chronostratigraphy

The Paks loess profile is located in the mid-Carpathian Basin on the right bank of the River Danube (46°38'24"N and 18°52'24"E, top of the sequence: ~135 m a.s.l.) (Fig. 1). According to drillings, the whole loess-paleosol series, underlain by a clay, silt, and red clay sequence called the Tengelic Red Clay Formation (Koloszár, 2004; Kovács et al., 2008, 2011), is ca. 60 m thick and represents approximately the last 1 Ma (Pécsi, 1979) (Fig. 2). Two lithologic units have been distinguished within the Paks Loess Formation: (1) the Young Loess Series (YLS; MIS 2-10) and (2) the Old Loess Series (OLS; MIS 11-22) (Pécsi, 1995; Gábris, 2007; see Fig. 2). Three loess layers and three rubefied brown forest soils (PDK, PD_2, PD_1) constitute the lower part of the OLS, while the upper part of OLS is represented by three loess layers, two brown forest soils (Phe_{1-2}, MB) and a pseudogley soil (Mtp) below the Phe_2 soil. As shown in Fig. 2, the PD_2 fossil soil was the lowermost paleosol that we could study in the exposure. Besides, four soil horizons were found in the stratigraphic position of Mtp and Phe

and we suppose that these paleosols are the Mtp_{1-2} and Phe_{1-2} soils of Pécsi et al. (1995). From chronological point of view, the position of the Matuyama-Brunhes Boundary (MBB) can be considered as the only reference point in the OLS. The MBB was found by Pécsi and Pevzner (1974) and Márton (1979) in a position below the PD_2 paleosol. Subsequently Sartori et al. (1999) and Sartori (2000) placed the MBB in the uppermost part of the PD_2 soil. Taking the potential depth offset between the measured and true positions of the MBB ('lock-in' depth, Zhou and Shackleton, 1999) into account, it is likely that the PD_2 soil can be correlated with MIS 19, and the older Pv_{1-3} and PDK paleosols formed during the Matuyama chron. It cannot be excluded, however, that the true position of the MBB is in the PD_1 soil (MIS 19), corresponding to the V-S7 soil in Serbia (Marković et al., 2011). Since the measured and true positions of the MBB are always linked to a loess-paleosol couplet and the MBB was found in the PD_2 or the underlying loess in the Paks section, this second 'scenario' is considered less likely. Correlation of the paleosols Mtp_{1-2} and Phe_{1-2} with the $\delta^{18}O$ curve (MIS 13-15) is heavily dependent on the position of the MBB, so it is only tentative and partly follows a recent work of Gábris (2007).

The Bag tephra, which we could trace only in the southern part of the Paks brickyard and could not be observed in the studied profile, is a widespread volcanological marker horizon in the YLS between the MB and BA soils. This tephra is another chronological tie point in spite of its age being poorly constrained (~350-380 to 788 ka, Pouclet et al., 1999; MIS 8 or 10, Horváth, 2001). Its proposed correlation with the Villa Senni Tuff, dated at around ~351 ka (Pouclet, et al., 1999), has been questioned in a recent study of Sági et al. (2008). In accordance with the published age (~351 ka) of the Bag tephra, the correlation of the bracketing paleosols with MIS 11 (MB soil) and with MIS 9 (BA soil) was independently proposed by Oches and McCoy (1995) based on amino acid racemization results, although further data would be needed to satisfactorily verify this highly likely scenario. Main findings

of TL dating frameworks (Wintle and Packmann, 1988; Singhvi et al., 1989; Zöller and Wagner, 1990; Zöller et al., 1994; Frechen et al., 1997) and an AAR study (Oches and McCoy, 1995), which were performed on the Mende, Basaharc and Paks sections, supported the idea of assigning the BD_{1-2} forest steppe soils to MIS 7a-e. Indeed, Frechen et al. (1997) published TL and IRSL ages of 100.5±9.8 to 167.9±17.2 from a loess layer overlying the BD_1 soil at Paks and they correlated the given loess layer with MIS 6. The chronostratigraphic position and correlation of MF_2 and MF_1 paleosols with MIS 5 and MIS 3 is nowadays well established based on the findings of TL and subsequent IRSL and AAR studies (Frechen et al., 1997; Novothny et al., 2002, 2009; Oches and McCoy, 2001). In contrast to the profile published by Pécsi et al. (1995) and Sartori et al. (1999) the MF_{1-2} soils were absent in the sequence we studied (Fig. 2).

3. Materials and methods

3.1. Sampling

A total of 36 loess and 28 paleosol samples were taken from the ~42 m thick Paks loess-paleosol section for mineralogical and geochemical analyses during 2009. Before sampling the profile was cleaned and samples were collected from the sequence at various depths given in Table 1. For paleosols, sampling points were placed relatively close to each other (20-30 cm) to get at least two data from each and every fossil soil horizon. The samples were numbered from top to bottom, so the numbering increases downwards in the profile (YLS sample codes: Pa-1 to Pa-32, OLS sample codes: Pa-33 to Pa-64).

131 *3.2. Analytical procedures and data processing*

132 *3.2.1. Bulk mineralogy*

133 Mineralogical analysis of the powdered bulk samples was performed at the Department of
134 Earth and Environmental Sciences of the University of Pannonia (Veszprém) by X-ray
135 powder diffraction (XRD), using a Philips PW 1710 diffractometer with CuKα radiation and
136 diffracted-beam graphite single-crystal monochromator.

137 Phases of the bulk rock specimens were identified from their characteristic reflections. Semi-
138 quantitative composition was estimated using integrated areas of 00*l* reflections (Moore and
139 Reynolds, 1997), i.e. ~15 Å peak for smectite and ~10 Å peak for illite. In order to resolve the
140 problem of superimposed peaks of kaolinite and chlorite ~7 Å in air-dried, non-oriented bulk
141 rock powder samples, areas of 3.58–3.59 Å peak of kaolinite and 3.54–3.55 Å peak of chlorite
142 were used. A correction factor of 2 for kaolinite (Bish, 1993) and that of 1.4 for chlorite
143 (Zanazzi et al., 2007) were applied for calculation.

144

145

146 *3.2.2. Bulk chemistry*

147 Loess and paleosol samples were analyzed for major and trace element abundances with X-
148 ray fluorescence spectrometry (XRF) using a Thermo ARL Advant'XP+ sequential XRF
149 spectrometer in the GeoAnalytical Laboratory of the Washington State University, Pullman,
150 WA, USA. After drying, samples were prepared for analysis by grinding to a very fine
151 powder, weighing with di-lithium tetraborate flux (2:1 flux:sample), fusing at 1000°C in
152 muffle oven and cooling. The bead is then reground, refused and polished on diamond laps to
153 provide a smooth flat analysis surface. The major element concentrations are expressed as
154 wt%, volatile-free, with all the iron expressed as FeO_{tot}. Loss on Ignition (LOI) was obtained
155 by weighing after 16 h of calcination at 900 °C. Analytical uncertainties are ± 2% for the

major elements (except Na_2O). Among the trace elements, the precision and therefore the accuracy of Ni, Cr, V, Sc, and Ba was lower than for Rb, Sr, Zr, Nb, Y, Ga, Cu, and Zn. Rb, Sr, Zr, Nb, Y, Pb, and Th had satisfactory precision and accuracy down to 1 to 3 ppm, while La and Ce data were less precise.

3.2.3. Paleoproxy indicators

A variety of semiquantitative and quantitative tools, including mineralogical and geochemical proxies, has been developed to examine past weathering and pedogenesis, and to reconstruct both paleoenvironmental and paleoclimatic conditions at the time of paleosol formation (e.g., Liu et al., 2005; Bokhorst et al., 2009; Sheldon and Tabor, 2009; Buggle et al., 2011). The concept of geochemical proxies of mineral alteration (i.e. weathering indices) relies on the selective removal of soluble and mobile elements from a weathering profile compared to the relative enrichment of rather immobile and non-soluble elements (Nesbitt and Young, 1982; Buggle et al., 2011). Based on this principle, simple ratios of bulk element composition together with chemical weathering indices have successfully been used for the reconstruction of paleoenvironmental conditions of loess–paleosol successions (e.g., Yang et al., 2006; Jeong et al., 2008; Muhs, et al., 2008; Bokhorst et al., 2009; Buggle et al., 2011; Varga et al., 2011). Recently, Buggle et al. (2011) and Varga et al. (2011) published some details of mineral and element behavior under weathering conditions, so this topic is not discussed here.

In this study, bulk kaolinite/illite (kao/ill), smectite/illite (sme/ill) and smectite/(illite+chlorite) [sme/(ill+chl)] ratios have been used as mineralogical proxy indicators (see Varga et al., 2011). Further, element ratios (Al_2O_3/Na_2O, K_2O/CaO, K_2O/Na_2O, MgO/TiO_2, Ba/Sr, Rb/Sr) have been applied for the geochemical characterization of Paks loess and paleosol samples. Major element weathering indices (in molar proportions) such as CIA ($CIA = Al_2O_3 / (Al_2O_3 + CaO^* + Na_2O + K_2O) \times 100$; Nesbitt and Young, 1982),

CIW (CIW = Al_2O_3 / (Al_2O_3 + CaO* + Na_2O) × 100; Harnois, 1988), and CIW' or CPA (CIW' = CPA = Al_2O_3 / (Al_2O_3 + Na_2O) × 100; Cullers, 2000; Buggle et al., 2011) have also been used for the reconstruction of paleoclimate and paleoenvironmental conditions during the deposition of the Paks loess record. In weathering indices, CaO* represents Ca in silicate-bearing minerals only. As we were not able to distinguish carbonate CaO from silicate CaO, the correction method of McLennan (1993) has been adapted which assums reasonable Ca/Na ratios in silicate minerals (see Buggle et al., 2008; Újvári et al., 2008; Varga et al., 2011).

4. Results

4.1. Bulk mineralogical composition

The bulk mineralogical composition of sediments, estimated from XRD data, indicates that quartz (~20–50%), smectite (~0–30% in loess and ~10–40% in paleosol), and carbonates are the dominant minerals (Fig. 3). Loess samples contain higher amounts of calcite (~5–30%) and dolomite (~5–25%) compared to paleosols which can be characterized by a smectite-dominance. Interestingly, in loess samples from the Paks YLS, smectite cannot be detected. Carbonate content of the YLS sediments is tendentiously higher than those of the OLS samples. Furthermore, the YLS loess samples are especially rich in dolomite (up to 25%). Illitic material (illite±muscovite) together with chlorite is present in all samples but usually in small proportion (<10%); YLS sediments, however, have a relatively higher bulk illite±muscovite and chlorite content (~5–20% and ~5–10%, respectively) compared to the OLS loess samples. Albite (~5–10%), K-feldspar (<5%), and amorphous material (~5–10%) are the typical minor components with a detectable amount of amphibole and kaolinite. Goethite is present in three samples in the lower part of the MB paleosol, whereas hematite occurs only in a single BA paleosol sample.

205 Paleoproxy indicators such as bulk kao/ill, sme/ill, and sme/(ill+chl) show systematic
206 variations with lithology (Fig. 3). These ratios in paleosols show higher values than in loess
207 samples. Furthermore, in the lower part of the Paks section (OLS), the sme/ill and
208 sme/(ill+chl) ratios in paleosols are significantly higher than in YLS fossil soils.
209
210 *4.2. Bulk chemical composition*
211 Major and trace element concentrations (volatile-free, wt%) are presented in Table 1. Loss on
212 ignition (LOI) ranges from 4.3 to 18.5% and shows a strong positive correlation with total
213 CaO and MgO (r = 0.98 and r = 0.88, respectively) in all samples. This suggests that LOI is
214 predominantly associated with carbonate minerals, but phyllosilicates and organic matter
215 could also play a minor role in the LOI budget.
216
217 *4.2.1. Major element abundances and their internal relationships*
218 Compositional variations among YLS loess samples (N=24) are low to moderate (Table 1).
219 They contain a relatively low and narrow range of SiO_2 from 58 to 69% (average: 62.6 ±
220 2.5%). Their Al_2O_3 and FeO contents also show narrow ranges from 9.4 to 13.5% and from
221 3.3 to 4.7%, respectively. On average, a relatively high TiO_2 content (0.8 ± 0.1%)
222 characterizes the YLS loess samples. MgO and CaO contents vary widely between 2.9 and
223 6.6% (average: 4.7 ± 1.0%) and between 7.2 and 18.4% (average: 13.3 ± 3.2%), respectively.
224 The YLS loess samples have low Na_2O and K_2O concentrations (1.2–1.6% and 1.7–2.3%,
225 respectively).
226 SiO_2 and Al_2O_3 contents of the YLS paleosol samples (N=8) show narrow ranges from 67 to
227 75% (average: 72.3 ± 3.3%) and from 11.7 to 14.0% (average: 13.0 ± 0.8%), respectively.
228 The YLS paleosol layers have relatively high TiO_2 (average: 0.94 ± 0.03%) and FeO contents
229 (average: 4.5 ± 0.3%). On average, CaO content is relatively low (average: 3.5 ± 2.5%) but

varies widely between 1.2 and 7.0%. Additionally, MgO, Na_2O, and K_2O contents are also low (1.6–2.5%, 1.3–1.6%, and 2.0–2.3%, respectively).

OLS loess (N=12) contains a wider range of SiO_2 from 59 to 76% (average: 65.3 ± 5.5%) relative to the YLS loess (Table 1). Al_2O_3 and FeO contents vary from 8.6 to 14.2% (average: 11.5 ± 1.5%) and from 2.8 to 4.8% (average: 4.0 ± 0.6%), respectively. TiO_2 contents range from 0.6 to 0.9%. MgO and CaO contents vary widely between 1.8 and 4.4% (average: 3.4 ± 0.9%) and between 4.3 and 16.0% (average: 11.4 ± 3.8%), respectively. However, these concentrations are somewhat lower than the same values in the YLS loess samples. The OLS loess samples also have low Na_2O and K_2O concentrations (1.1–1.5% and 1.7–2.5%, respectively).

In the OLS paleosol samples (N=20), a heterogeneous chemical composition is apparent (Table 1). SiO_2 content varies widely between 61.2 and 80.9% (average: 70.6 ± 5.1%). In addition, CaO content also shows a wide range with values between 1.1 and 15.0% (average: 6.1 ± 3.1%). Nevertheless, other major elements have a less pronounced variation. Al_2O_3 and FeO contents range from 8.8 to 14.5% and from 2.9 to 5.1%, respectively. TiO_2 contents range from 0.7 to 1.0%. MgO, Na_2O, and K_2O contents are relatively low showing a little variation between 0.9–2.4%, 0.8–1.5%, and 1.6–2.3%, respectively.

In general, SiO_2 content does not systematically vary with Al_2O_3 (Fig. 4a). The lack of significant relationships ($|r|$ = 0.9 or higher) between SiO_2 and Al_2O_3 strongly suggests that absolute concentrations of the major elements are affected by cumulative effects of several factors such as carbonate and quartz dilution and closed sum effect. Further, SiO_2 and Al_2O_3 concentrations plot close to the composition of slightly weathered crustal rocks such as the Upper Continental Crust (UCC; Rudnick and Gao, 2003) and the Global Average Loess (GAL; Újvári et al., 2008), whereas samples plot far from relatively altered sedimentary deposits like the post-Archean Australian average shale (PAAS; Taylor and McLennan,

1985). There is no significant linear correlation between SiO_2 and TiO_2 for the Paks samples (Fig. 4b). The scattered distribution of the SiO_2 – TiO_2 datapairs in this figure is likely to be caused by a dual emplacement of Ti in silicates (e.g., chlorite and amphibole) and oxides (e.g., rutile). In the K_2O vs. Al_2O_3 compositional space (Fig. 4c) samples plot close to GAL. In general, the clear relationship between these elements (r = 0.94, N=64) suggests that Al_2O_3 abundance is mainly governed by the presence of phyllosilicates (especially, illitic material) and/or K-feldspar. In the diagram of Na_2O/Al_2O_3 vs. K_2O/Al_2O_3 (Fig. 4d), both YLS and OLS loess samples cluster near the GAL composition. This is considered diagnostic of depositional conditions of sedimentary rocks which have distinctly lower Na_2O/Al_2O_3 values than igneous rocks (Garrels and MacKenzie, 1971; Gallet et al., 1998). Further, the even lower Na_2O/Al_2O_3 values in paleosols compared to loess samples (especially in the OLS paleosols) refer to the advanced stage of sodium mobilization during pedogenesis.

4.2.2. UCC-normalized major and trace element fingerprints

The SiO_2, Al_2O_3, FeO, MnO, and K_2O contents of the YLS samples are similar or slightly lower than those of the UCC and they are slightly enriched in TiO_2 and P_2O_5 (Fig. 5a). On the other hand, all YLS samples are strongly depleted in Na_2O relative to the UCC. High MgO and CaO concentrations are characteristic of the Paks YLS loess samples, whereas YLS paleosols are mostly depleted in CaO and MgO compared to the UCC. The trace element distribution is less variable among the YLS samples than major-element data (Fig. 5a), only Sr and U contents show wider ranges (Table 1). All samples have similar (or slightly higher) concentrations of Rb, Th, and Nb compared to UCC and they are depleted in Ba, Sr, Cr, and V. Further, the YLS samples are enriched in U, Y, and Zr relative to the UCC.

In general, OLS samples have a similar UCC-normalized major and trace element distribution as YLS samples have (Fig. 5); however, their patterns display more pronounced variations (e.g., MgO, CaO, Th, and U values). Regarding the P_2O_5 composition, it is important to note that three OSL paleosol samples are significantly depleted in this major element compared to the UCC (Fig. 5b).

4.2.3. Al_2O_3–CaO+Na_2O–K_2O (A–CN–K) relationships and other chemical proxies of weathering*

In the Al_2O_3–CaO*+Na_2O–K_2O (A–CN–K) diagram (Nesbitt and Young, 1984), the Paks samples plot closely together along a line parallel to the A–CN join (Fig. 6). This is a typical distribution of sediments having been subjected to different degree of chemical weathering, resulting in a predominant removal of silicatic Ca and Na due to the destruction of plagioclase feldspars (Nesbitt and Young, 1982, 1984). In the studied Paks section, CIA values are in the range of 60–71, which are higher than the UCC and GAL values of 53 and 60 (Rudnick and Gao, 2003; Újvári et al., 2008) and slightly lower than the PAAS value of 70 (Taylor and McLennan, 1985). The CIA values of YLS loess samples range from 60 to 64 (average: 62±1) and for YLS paleosol samples from 64 to 68 (average: 66±1). The OLS samples have slightly higher CIA values which vary from 61 to 66 (average: 64±2) in loess samples and from 61 to 71 (average: 68±1) in paleosols (Table 1).

At Paks, all applied simple ratios of bulk chemical element composition and weathering indices reflect the lithology (Fig. 7). Higher values of Al_2O_3/Na_2O, K_2O/CaO and K_2O/Na_2O ratios together with lower values of MgO/TiO_2 ratios in paleosols compared to loess samples reflect intense carbonate and weak to moderate silicate dissolution during post-depositional processes. Changes of Ba/Sr and Rb/Sr ratios are almost perfectly parallel to that of K_2O/CaO record, implying that these variations are also due to chemical, especially carbonate

weathering. Paleosol samples show higher CIA, CIW, CIW' (CPA), and lower ($CaO^*+Na_2O+MgO)/TiO_2$ (Yang et al., 2006) values than intervening loess does, indicating stronger weathering of fossil soils. It is worthwile to note that all weathering ratios and indices, except for TiO_2-normalized ones, display a slight decrease from the OLS to the YLS (Fig. 7).

5. Discussion

5.1. Implications for provenance

The elements Th and Zr are enriched in felsic rather than in mafic rocks, because they are highly incompatible during most igneous melting and fractionation processes (Taylor and McLennan, 1985; McLennan, 2001). The Zr/V and Zr/Ni ratios are useful proxies of zircon enrichment since Zr is enriched in zircon, whereas V and Ni generally preserves a signature of the provenance. At the same time, Th/V and Th/Ni are good overall indicators of igneous chemical differentiation processes since Th is incompatible, whereas V and Ni are typically compatible elements in igneous systems (McLennan et al., 1993). Thus, heavy mineral (e.g., zircon, monazite) enrichment due to sedimentary sorting and recycling has been tested using Zr/V vs. Th/V, and Zr/Ni vs. Th/Ni diagrams (see Újvári et al., 2008). In these diagrams data intersect a primary compositional trend (dashed line with arrow) defined by igneous rocks (Condie, 1993) at high Zr/metal ratio, above the average value of UCC and PAAS, corresponding to the GAL composition and the upper limit of the 'Floodplain sediments' field (Figs. 8a and 8b). High Zr/metal ratios clearly demostrate zircon enrichment in loess and paleosol samples of Paks compared to UCC, PAAS and Hungarian floodplain sediments, implying that aeolian (or combined fluvial-aeolian?) transport efficiently concentrates zircon minerals. At the same time, Th/metal ratios show only minor variability which is interpreted to be due to negligible compositional variations of provenance and suggests stable felsic

sources for the Paks sediments over the last 0.8 Ma. This observation is further supported by the enrichment of TiO_2, Y and Zr, and the depletion of Al_2O_3, Fe_2O_3, K_2O, Na_2O, Ba, Sr, Cr and V compared to the UCC (Fig. 5) and the fact that the loess and paleosol samples plot along a straight line (weathering trend) starting from an unweathered (granodioritic) source composition in the A-CN-K diagram pointing towards the composition of Hungarian red clays (Fig. 6), which are also thought to be aeolian in origin (Kovács et al., 2011). Any dispersion and/or trend in the data (from loess to paleosols) are attributed to chemical weathering. The inference concerning a stable provenance for loesses and paleosols in the Paks section demostrated by the Zr/V vs. Th/V, Zr/Ni vs. Th/Ni and UCC-normalized major and trace element diagrams is further supported by a previous study on the heavy minerals of the Paks section. Szebényi (1979) revealed that the different cycles of loess deposition in the profile over the last 0.8 Ma can be characterized by very similar heavy mineral assemblages and concluded that the material of loess may have experienced only a short transport and originated from a stable source. Amphiboles (in general) detected by our XRD measurements and hornblendes reported by Szebényi (1979), as well as high amounts of detrital dolomite and zircon U-Pb ages (Újvári et al., in press) also refer to the partly local origin of loess material.

In the Ni vs. TiO_2 space (Fig. 8c), loess and paleosol samples cluster at the upper margin of the field of acidic rocks and 'Floodplain sediments', and plot close to GAL. The TiO_2 values of the Paks sediments are generally higher than those in most acidic rocks, while the Ni values are well within the range characteristic for acidic rocks. The higher TiO_2 values can be explained by Ti-bearing heavy mineral enrichment (e.g. rutile, titanite) resulting from sedimentary sorting and recycling. Higher Y/Ni and similar Cr/V ratios were found in the loesses and paleosols from Paks compared to the UCC (Fig. 8d). Since mafic rocks have high ferromagnesian trace element abundances (low Y/Ni and high Cr/V in ultramafic rocks) and

lower abundances of compatible elements such as Cr, V and Ni in the Paks sediments were found, a contribution from mafic/ultramafic sources to the Paks sediments seems to be insignificant (Fig. 8c and d). At the same time, these provenance diagrams suggest that sediments in the Paks section may have been derived from floodplain sediments, or at least a genetic link between these materials seems to be likely. This observation is consistent with previous findings of Buggle et al. (2008) and Újvári et al. (2008) and suggest that the relation to floodplain sediments is a general feature of loess deposits in the Carpathian Basin.

5.2. Weathering, pedogenesis and mineralogical-geochemical proxy variations

Relative abundance of smectite and the sme/ill ratio is significantly lower in loess samples relative to paleosol samples (Fig. 3), suggesting clear fluctuations in weathering intensity during the evolution of the studied sequence. Additionally, relative abundances of smectitic material is higher in paleosols, whereas illite (illite±muscovite) content is higher in loess. The apparent inverse behaviour of illitic material and smectite in the depth profile can indicate transformation of illite into smectitic material in periods of soil formation.

Other authors have also noted large amounts of illite, smectite (especially in paleosols) and dolomite (especially in the YLS loess) with heterogeneous distribution in the Paks section (Pécsi-Donáth, 1979; Nemecz et al., 2000). In loess, muscovite and chlorite have been enriched in the coarser grain-size-fractions, suggesting a predominantly detrital origin for these minerals, whereas smectite and rare kaolinite have been documented exclusively in the finer fractions (Nemecz et al., 2000), indicating their diagenetic origin. Consequently, illite and chlorite is considered here as mainly primary minerals so they are thought to be representative of physical erosion. Their dominance in a sample indicates relatively fast erosion and also cold and/or dry climatic conditions of the source areas (Weaver, 1989; Varga et al., 2011 and references therein). Further, smectite is considered to be an *in situ* product of

weak to moderate weathering of illite±muscovite and of other detrital phases (especially albite) at both source and depositional sites. Therefore, sme/ill and sme/(ill+chl) ratios were used here as clay mineralogical indicators of the chemical weathering versus physical erosion history (see Liu et al., 2005; Varga et al., 2011).

In the Paks section, variations of mineralogical and geochemical proxies show similar general trends (Figs. 3, 6 and 7). Higher smectite content together with higher values of mineralogical ratios and weathering indices (CIA, CIW, CIW'/CPA) observed in paleosols, suggest strengthened chemical weathering and weak physical erosion during soil forming phases. By contrast, lower ratios in loesses refer to intensified physical erosion and weakened chemical weathering. Additionally, all of the applied paleoproxy indicators reveal decreasing weathering intensity from the OLS to the YLS (Figs. 3 and 7), reflecting moderate (regarding loess) to intense (regarding paleosol) chemical weathering during the deposition of the OLS but weak (in loess) to moderate (in paleosol) weathering during the deposition of the YLS at the Paks section. A similar observation was made in the Beremend section by Varga et al. (2011), but the difference in the magnitude of weathering between the two loess series (OLS vs. YLS) has been more pronounced there owing to frequent apperance of erosion layers in the profile.

In general, weathering of primary silicates such as albite results in the formation of clay minerals like montmorillonite which belongs to the smectite group. For montmorillonite, the presence of Mg^{2+} (leached e.g. from dolomite, pyroxenes, amphiboles or biotite) is assumed (Appelo and Postma, 2009):

$$3Na(AlSi_3)O_8 + Mg^{2+} + 4H_2O \rightarrow 2Na_{0.5}(Al_{1.5}Mg_{0.5})Si_4O_{10}(OH)_2 + 2Na^+ + H_4SiO_4$$

Mineralogy of the Paks samples, including albite and amphibole in loess and abundant smectite in paleosol, reflect a weathering process described by the equation above during

404 pedogenesis. The presence of amphibole and biotite in the whole loess-paleosol profile at
405 Paks is also supported by the heavy mineral analyses of Szebényi (1979).
406 Regarding hydrological conditions, smectite is preferentially formed under relatively dry
407 climates with low rainfall, where the rate of flushing of the soil is low, so that the solute
408 concentrations become higher (Weaver, 1989; Appelo and Postma, 2009). It is worthwile to
409 note, however, that the relative abundance of smectite in paleosols is constant (up to 30–40%)
410 throughout the entire section (Fig. 3) and no authigenic kaolinit formation could be observed,
411 suggesting the same degree of chemical weathering for both OLS and YLS interglacials. On
412 the other hand, the higher proportion of inherited phyllosilicates (illite and chlorite) in the
413 YLS samples relative to the OLS may suggest that only the magnitude of physical erosion
414 was higher in the source area with a relatively high relief. In theory, this would mean that the
415 decreasing values of chemical weathering indices (CIA, CIW, CIW'/CPA) are just artifacts of
416 enhanced physical erosion and resulting dust deposition.
417
418
419
420 *5.3. Mechanisms behind the 10^5-10^6-year scale trend of chemical weathering: progressive*
421 *aridization, changing sedimentation rates or tectonic effects?*
422 Five main factors are considered controlling soil and, consequently, paleosol development:
423 climate, parent material, organisms, topographic relief, and time (Alonzo-Zarza, 2003 and
424 references therein). Each of these factors has a recognisable effect on the soil, so it is possible
425 to understand the complex and multiple processes that operate during pedogenesis. In general,
426 a close relationship between climate and paleosol formation has been recognised (Weaver,
427 1989; Bokhorst et al., 2009; Sheldon and Tabor, 2009; Stevens et al., 2011), despite the fact
428 that climate is just one soil forming factor among the others. At present, there are soils with

similar parent materials, developed under similar climates but with different characteristics related to variations in topographic relief and drainage (e.g. catenas). When it is possible to isolate other allogenic factors, tectonism also exerts a control on paleosol characteristics by having an influence on sedimentation rates and by generating different geomorphic settings (relief). In continental basins, tectonism seems to be the main agent responsible for generating space for deposition, and thus it controls the long-term stratigraphic signal (Alonzo-Zarza, 2003; Varga et al., 2011). Finally, the degree of paleosol development is clearly controlled by the time it has had to form (Alonzo-Zarza, 2003; Sheldon and Tabor, 2009).

The proxy data above demonstrate the complexity of the environmental signal at the study site; however, provenance (parent material) changes can be excluded. A general trend of decreasing chemical weathering intensity in the Paks loess-paleosol section is unequivocal as demostrated by weathering proxies such as CIA or CIW (Fig. 7). Pedogenetic intensity likewise changed in the profile from the oldest, well-developed rubefied brown forest soils (PD_{1-2}) (CIA: 68-71) to degraded chernozems of BD_{1-2} (CIA: ~64) likely reflecting a decreasing moisture availability. Similar trends in chemical weathering and pedogenesis were observed in other loess profiles in the Carpathian Basin (Batajnica and Stari Slankamen, Serbia: Marković et al, 2009; Buggle et al., 2010; Beremend, Hungary: Varga et al., 2011), reflecting that the recorded trend is regional. The decreasing intensity of chemical weathering can be accounted for in two different ways: (1) by lowered maturity of clastic material, and (2) by decreased post-depositional weathering intensity (Yang et al., 2006; Buggle et al., 2010; Varga et al., 2011). The first explanation is closely related to tectonism in and around the sedimentary basin, as higher and higher uplift rates result in increasing erosion, providing high amounts of fresh, unweathered material to loess deposition. Indeed, increasing amounts of detrital carbonates and layer silicates (chlorite and illit±muscovite) in the Paks sequence from the OLS to YLS refer to enhanced mechanical erosion, implying increased denudation in

454 the mountains in and around the sedimentary basin and related enhanced sediment input of the
455 depositional region. The second explanation, namely the lowered post-depositional
456 weathering may result from two interrelated processes, cooling and drying of climate in the
457 depositional region and increased dust sedimentation rates. As a matter of fact, a gradual
458 decrease of paleoprecipitation in Southeastern Europe from the Middle to the Late Pleistocene
459 was recorded by Buggle et al. (2009). Further, the Tenaghi Pilippon pollen record in Greece
460 revealed a major shift in the vegetational composition of interglacials with forest becoming
461 dominated by drought tolerant taxa after MIS 16 (the end of the Mid-Pleistocene Transition,
462 MPT) which can partly be explained by a shift towards more arid interglacial conditions
463 (Tzedakis et al., 2006). At the same time, an enhanced dust deposition is thought to be the
464 'by-product' of aridization and increasing wind strength which yields fresh, less weathered
465 material to loess and paleosols thereby causing a dilution effect and eventually lower CIA
466 values (Yang et al., 2006; Varga et al., 2011). Indeed, the increasing thickness of loess layers
467 towards the YLS in the Paks section can be considered as an indication of intensifying dust
468 flux and loess sedimentation during the succession of glacial cycles. Further, smectite
469 abundances are stable (30–40%) in both older and younger paleosols, so decreasing sme/ill
470 ratios in paleosols from the OLS to YLS resulted from an increase of illite contents. This
471 reflects progressive enhancement of physical erosion and the deposition of more and more
472 unweathered material (higher sedimentation rates) and does not represent an aridization
473 process. Shorter periods of pedogenesis, reflected in the lower thickness of younger paleosols,
474 and permanent dust accretion of these soils during pedogenesis can explain lower CIA values.
475 This conclusion is also supported by the study of Bronger (2003) who emphasized that much
476 greater pedochemical weathering and clay mineral formation of some older fossil soils results
477 from a longer period of pedogenesis and does not indicate a wetter or warmer climate.

As there are evidences for all three mechanisms (climate and tectonic forcing, enhanced dust deposition; see e.g. Varga et al., 2011) and we are unable to unmix the composite signal of weathering from source regions and depositional areas, further work is needed (with more independent and/or sophisticated proxies) to gain a better understanding of processes behind chemical weathering trends in loess-paleosol archives in Eurasia.

6. Conclusions

The Paks loess-paleosol sequence, spanning the last 0.8 Ma and as being one of the most important archives of Quaternary environmental change in East Central Europe, was investigated in the present study from mineralogical and geochemical points of view. Proxies generated from these data are controlled by physical erosion and chemical weathering as a result of the interplay of tectonism, climate and time. While geochemical indices (CIA, CIW, CIW'/CPA) showed a general decreasing trend of chemical weathering, mineralogical data (dolomite content) and ratios (e.g. sme/ill) revealed a gradient of increasing physical erosion and does not demonstrated significant changes in climate over the last 0.8 Ma. In theory, the observed chemical weathering trend can be explained by enhanced input of relatively unweathered material and by climate deterioration during the Quaternary. The applied proxies allowed us to draw the conclusion that enhanced physical erosion of the source areas, driven by tectonism, increasing dust sedimentation at the depositional site and the duration of soil formation are the main factors of controlling chemical weathering in the profile. Despite the fact that clay mineralogical data from the Paks loess-paleosol sequence do not provide evidence for progressive aridization of this region, an increasing loess sedimentation in response to raising wind strength reflecting paleoclimate change cannot be dismissed. As these mineralogical data are only semi-quantitative, further work is needed (with more sophisticated proxies) to gain a deeper insight into these concurrent processes (tectonic and

503 climatic forcing) which eventually determine the final value of any chemical weathering
504 indices (CIA, CIW, CIW'/CPA). Bearing these facts in mind and as the paleosols can be
505 distinguished based on their geochemistry in the Paks profile we propose a framework for the
506 regional chemical correlation of fossil soils in the Carpathian Basin complemented with their
507 micromorphology and mineralogy.
508 Regrading the provenance of the clastic material of the Paks sediments, felsic sources
509 primarily contributed mineral particles to loess deposition and there is no detectable change in
510 provanenance over the 0.8 Ma. Lower abundances of compatible elements like Cr, V and Ni
511 in loesses and paleosols in the Paks profile highlight the fact that the proportions of mafic or
512 ultramafic rocks were insignificant in the source area(s). Mineralogical and geochemical
513 considerations (presence of amphibole, hornblende; detrital dolomite content and zircon U-Pb
514 ages) refer to a partly local origin of loess material and a link between floodplain sediments
515 and loess in the basin.
516

517 **Acknowledgments**

518 We wish to thank László Merényi for his help with sample preparations (XRD) and Richard
519 M. Conrey and Laureen C. Wagoner (GeoAnalytical Lab, WSU, USA) for the XRF
520 measurements. This research has been supported by the Hungarian-American Fulbright
521 Commission Research Grant to GÚ (Grant number: 1209105), and it was additionally
522 supported by the 'Developing Competitiveness of Universities in the South Transdanubian
523 Region (SROP-4.2.1.B-10/2/KONV-2010-0002)' project (BR and JK) as well as the Bolyai
524 János Research Scholarship of the Hungarian Academy of Sciences (GÚ and JK). Valuable
525 comments of the two anonymous reviewers are highly appreciated.
526

527 **References**

528 Alonso-Zarza, A.M., 2003. Palaeoenvironmental significance of palustrine carbonates and
529 calcretes in the geological record. Earth-Science Reviews 60, 261–298.
530 Amorosi, A., Centineo, M.C., Dinelli, E., Lucchini, F., Tateo, F., 2002. Geochemical and
531 mineralogical variations as indicators of provenance changes in late quaternary deposits of
532 SE Po Plain. Sedimentary Geology 151, 273–292.
533 Appelo, C.A.J., Postma, D., 2009. Geochemistry, groundwater and pollution, 2nd edition, CRC
534 Press, Fourth corrected reprint, 649 p.
535 Bish, D.L., 1993. Rietveld refinement of the kaolinite structure at 1.5 K. Clays and Clay
536 Minerals 41, 738–744.
537 Bokhorst, M.P., Beets, C.J., Marković, S.B., Gerasimenko, N.P., Matviishina, Z.N., Frechen, M.,
538 2009. Pedo-chemical climate proxies in late Pleistocene Serbian-Ukranian loess sequences.
539 Quaternary International 198, 113–123.
540 Bronger, A., 2003. Correlation of loess-paleosol sequences in East and Central Asia with SE
541 Central Europe - towards a continental Quaternary pedostratigraphy and paleoclimatic
542 history. Quaternary International 106–107, 11–31.
543 Buggle, B., Glaser, B., Zöller, L., Hambach, U., Marković, S., Glaser, I., Gerasimenko, N., 2008.
544 Geochemical characterization and origin of Southeastern and Eastern European loesses
545 (Serbia, Romania, Ukraine). Quaternary Science Reviews 27, 1058–1075.
546 Buggle, B., Hambach, U., Glaser, B., Gerasimenko, N., Markovic, S., Glaser, I., Zöller, L., 2009.
547 Stratigraphy, and spatial and temporal paleoclimatic trends in South-eastern/Eastern
548 European loess paleosol sequences. Quaternary International 196, 86–106.
549 Buggle, B., Kehl, M., Hambach, U., Markovic, S.B., Bruno, G., 2010. Progressive aridization
550 of the middle and lower Danube Basin since the lower Pleistocene, In: Lassu, T. (Ed.),
551 International Workshop on Loess Research and Geomorphology, Pécs, Hungary, Book
552 of Abstracts, p. 8.

553 Buggle, B., Glaser, B., Hambach, U., Gerasimenko, N., Markovič, S.B., 2011. An evaluation
554 of geochemical weathering indices in loess-paleosol studies. Quaternary International
555 240, 12–21.
556 Condie, K.C., 1993. Chemical composition and evolution of the upper continental crust:
557 Contrasting results from surface samples and shales. Chemical Geology 104, 1-37.
558 Cullers, R.L., 2000. The geochemistry of shales, siltstones and sandstones of Pennsylvanian-
559 Permian age, Colorado, USA: implications for provenance and metamorphic studies.
560 Lithos 51, 181–203.
561 Fink, J., Kukla, G.J., 1977. Pleistocene climates in central Europe: At least 17 interglacials
562 after the Olduvai event. Quaternary Research 7, Pages 363–371.
563 Floyd, P.A., Winchester, J.A., Park, R.G., 1989. Geochemistry and tectonic setting of Lewisian
564 clastic metasediments from the early Proterozoic Loch Maree Group of Gairloch, N. W.
565 Scotland. Precambrian Research 45, 203–214.
566 Frechen, M.A., Horváth, E., Gábris, Gy., 1997. Geochronology of middle and upper
567 Pleistocene loess sections in Hungary. Quaternary Research 48, 291–312.
568 Gallet, S., Jahn, B., Van Vliet Lanoë, B., Dia, A., Rossello, E., 1998. Loess geochemistry and
569 its implications for particle origin and composition of the upper continental crust.
570 Earth and Planetary Science Letters 156, 157–172.
571 Garrels, R.M., Mackenzie, F.T., 1971. Evolution of Sedimentary Rocks. Norton & Company,
572 New York, p. 397.
573 Gábris, Gy., 2007. Kapcsolat a negyedidőszaki felszínalakító folyamatok időrendje és az
574 oxigén-izotóp-rétegtan között – magyarországi lösz-paleotalaj-sorozatok és folyóvízi
575 teraszok példáján (The relation between the time scale of the Quaternary surface
576 processes and oxygen isotope stratigraphy – according to the loess-paleosoil sequences
577 and river terraces in Hungary). Földtani Közlöny 137, 515–540.

578 Gibbard, P., Cohen, K.M., 2008. Global chronostratigraphical correlation table for the last 2.7
579 million years. Episodes 31, 243–247.
580 Harnois, L., 1988. The CIW index: A new chemical index of weathering. Sedimentary
581 Geology 55, 319–322.
582 Hiscott, R.N., 1984. Ophiolitic source rocks for Taconic-age flysch: trace-element evidence.
583 GSA Bulletin 95, 1261–1267.
584 Horváth, E., 2001. Marker horizons in the loesses of the Carpathian Basin. Quaternary
585 International 76/77, 157–163.
586 Jámbor, Á., 1997. Tengelici Vörösagyag Formáció (The Tengelic Red Clay Formation). In:
587 Császár, G. (Ed), Basic lithostratigraphic units of Hungary, charts and short
588 descriptions. Magyarország Litosztratigráfiai Alapegységei, Táblázatok és rövid
589 leírások. MÁFI, Bp., 114 p.
590 Jeong, G.Y., Hillier, S., Kemp, R.A., 2008. Quantitative bulk and single-particle mineralogy
591 of a thick Chinese loess–paleosol section: implications for loess provenance and
592 weathering. Quaternary Science Reviews 27, 1271–1287.
593 Jordanova, D., Petersen, N., 1999. Paleoclimatic record from a loess-soil profile in
594 northeastern Bulgaria II. Correlation with global climatic events during the
595 Pleistocene. Geophysical Journal International 138, 533–540.
596 Jordanova, D., Hus, J., Geerarts, R., 2007. Palaeoclimatic implications of the magnetic record
597 from loess/palaeosol sequence Viatovo (NE Bulgaria). Geophysical Journal
598 International 171, 1036-1047.
599 Kemp, R.A., 2001. Pedogenic modi fi cation of loess: signi fi cance for palaeoclimatic
600 reconstructions. Earth Science Reviews 54, 145–156.
601 Koloszár, L., 2004. A Tengelici Formáció kifejlődései a DK-Dunántúlon. (Developments of
602 the Tengelic Formation in South-east Transdanubia) Földtani Közlöny 134, 345–369.

603 Koloszár, L., 2010. The thickest and the most complete loess sequence in the Carpathian
604 basin: the borehole Udvari-2A. Central European Journal of Geosciences 2, 165–174.
605 Kovács, J., Varga, Gy., Dezső, J., 2008. Comparative study on the Late Cenozoic red clay
606 deposits from China and Central Europe (Hungary). Geological Quarterly 52, 369–
607 382.
608 Kovács, J., Fábián, Sz.Á., Varga, G., Újvári, G., Varga, Gy., Dezső, J., 2011. Plio-Pleistocene
609 red clay deposits in the Pannonian basin: A review. Quaternary International 240, 35–
610 43.
611 Lisiecki, L.E., Raymo, M., 2005. A Pliocene-Pleistocene stack of 57 globally distributed
612 benthic d18O records. Paleoceanography 20, PA1003. doi:10.1029/2004PA001071.
613 Liu, Z., Colin, C., Trentesaux, A., Siani, G., Frank, N., Blamart, D., Farid, S., 2005. Late
614 Quaternary climatic control on erosion and weathering in the eastern Tibetan Plateau
615 and the Mekong Basin. Quaternary Research 63, 316–328.
616 Marković, S.B., Hambach, U., Catto, N., Jovanović, M., Buggle, B., Machalett, B., Zöller, L.,
617 Glaser, B., Frechen, M., 2009. The middle and late Pleistocene loess-palaeosol
618 sequences at Batajanica, Vojvodina, Serbia. Quaternary International 198, 255–266.
619 Marković, S.B., Hambach, U., Stevens, T., Kukla, G.J., Heller, F., McCoy, W.D., Oches,
620 E.A., Buggle, B., Zöller, L., 2011. The last million years recorded at the Stari
621 Slankamen (Northern Serbia) loess-palaeosol sequence: revised chronostratigraphy
622 and long-term environmental trends. Quaternary Science Reviews 30, 1142–1154.
623 Márton, P., 1979. Paleomagnetism of the Paks brickyard exposures. Acta Geologica
624 Hungarica 22, 443–449.
625 McLennan, S.M., 2001. Relationships between the trace element composition of sedimentary
626 rocks and upper continental crust. Geochemistry, Geophysics, Geosystems 2, 24,
627 2000GC000109.

McLennan, S.M., Hemming, S., McDaniel, D.K., Hanson, G.N., 1993. Geochemical approaches to sedimentation, provenance and tectonics. In: Johnsson, M.J., Basu, A. (Eds.), Processes Controlling the Composition of Clastic Sediments, Geological Society of America Special Paper, 284, pp. 21–40.

Moore, D.M., Reynolds, R.C. Jr., 1997. X-Ray Diffraction and the Identification and Analysis of Clay Minerals. Oxford University Press, Oxford. 378 p.

Muhs, D.R., Bettis, E.A., Aleinikoff, J.N., McGeehin, J.P., Beann, J., Skipp, G., Marshall, B.D., 2008. Origin and paleoclimatic significance of Quaternary loess in Nebraska: Evidence from stratigraphy, chronology, sedimentology, and geochemistry. Geological Society of America Bulletin 120, 1378–1407.

Nemecz, E., Pécsi, M., Hartyáni, Zs., Horváth, T., 2000. The origin of the silt size quartz grains and minerals in loess. Quaternary International 68–71, 199–208

Nesbitt, H.W., Young, G.M., 1982. Early Proterozoic climates and plate motions inferred from major element chemistry of lutites. Nature 299, 715–717..

Nesbitt, H.W., Young, G.M., 1984. Prediction of some weathering trends of plutonic and volcanic rocks based on thermodynamic and kinetic considerations. Geochimica et Cosmochimica Acta 48, 1523–1534.

Novothny, Á., Horváth, E., Frechen, M., 2002. The loess profile at Albertirsa, Hungary – improvements in loess stratigraphy by luminescence dating. Quaternary International 95/96, 155–163.

Novothny, Á., Frechen, M., Horváth, E., Bradák, B., Oches, E.A., McCoy, W.D., Stevens, T., 2009. Luminescence and amino acid racemization chronology of the loess–paleosol sequence at Süttő, Hungary. Quaternary International 198, 62–76.

Oches, E.A., McCoy, W.D., 1995. Amionostratigraphic evaluation of conflicting age estimates for the „Young Loess" of Hungary. Quaternary Research 44, 160–170.

653 Oches, E.A., McCoy, W.D., 2001. Historical developments and recent advances in amino acid
654 geochronology applied to loess research: examples from North America, Europe, and
655 China. Earth-Science Reviews 54, 173–192.
656 Pécsi-Donáth, É., 1979. Thermal investigation of the loesses and fossil soils of Paks. Acta
657 Geologica Hungarica 22, 419–426.
658 Pécsi, M., 1979. Lithostratigraphical subdivision of the loess profiles at Paks. Acta Geologica
659 Hungarica 22, 409–418.
660 Pécsi, M., 1985. Chronostratigraphy of Hungarian loesses and the underlying subaerial
661 formation. In: Pécsi, M., (Ed.), Loess and the Quaternary, Studies in Geography in
662 Hungary 18, pp. 33–49.
663 Pécsi, M., 1995. Loess stratigraphy and Quaternary climatic change. In: Pécsi, M.,
664 Schweitzer, F. (Eds.), Concept of loess, loess-paleosol stratigraphy. Loess inForm 3,
665 pp 23–30.
666 Pécsi, M., 1998. Lösz- és őstalajsorozatok és a negyedidőszaki ősföldrajzi változások
667 kutatásának elvi, módszertani kérdései (Loess-paleosol series and theoretical,
668 methodological issues in the research of Quaternary paleogeographical variations). In:
669 Haas, J. (Ed.), Fülöp József-emlékkönyv, Akadémiai Kiadó, Budapest, pp. 263–279.
670 Pécsi, M., Pevzner, M.A., 1974. Paleomagnetic measurements in the loess sequences at Paks
671 and Dunaföldvár, Hungary. Földrajzi Közlemények 22, 215-219.
672 Pécsi, M., Schweitzer, F., Balogh, J., Balogh, M., Havas, J., Heller, F., 1995. A new loess–
673 paleosol lithostratigraphical sequence at Paks, Hungary. Loess inForm 3, 63–78.
674 Pouclet, A., Horváth, E., Gábris, Gy., Juvigné, E., 1999. The Bag Tephra, a widespread
675 tephrochronological marker in Middle Europe: chemical and mineralogical
676 investigations. Bulletin of Volcanology 60, 265–272.

677 Rudnick, R.L., Gao, S., 2003. Composition of the continental crust. In: Holland, H.D.,
678 Turekian, K.K. (Eds.), Treatise on Geochemistry 3, Elsevier-Pergamon, Oxford-
679 London, 1–64.
680 Salminen, R., Batista, M. J., Bidovec, M., Demetriades, A., De Vivo, B., De Vos, W., Duris,
681 M., Gilucis, A., Gregorauskiene, V., Halamic, J., Heitzmann, P., Lima, A., Jordan, G.,
682 Klaver, G., Klein, P., Lis, J., Locutura, J., Marsina, K., Mazreku, A., O'Connor, P. J.,
683 Olsson, S.Å., Ottesen, R.-T., Petersell, V., Plant, J.A., Reeder, S., Salpeteur, I.,
684 Sandström, H., Siewers, U., Steenfelt, A., Tarvainen, T., 2005. Geochemical Atlas of
685 Europe. Part 1: Background Information, Methodology and Maps. Espoo, Geological
686 Survey of Finland. http://www.gsf.fi/publ/foregsatlas/ForegsData.php, last accessed:
687 28 September 2011.
688 Sartori, M., 2000. The Quaternary climate in loess sediments: Evidence from rock and
689 mineral magnetic and geochemical analysis. PhD thesis, ETH Zürich, p. 231.
690 Sartori, M., Heller, F., Forster, T., Borkovec, M., Hammann, J., Vincent, E., 1999. Magnetic
691 properties of loess grain size fractions from the section at Paks (Hungary). Physics of
692 the Earth and Planetary Interiors 116, 53–64.
693 Sági, T., Kiss, B., Bradák, B., Harangi, Sz., 2008. Középső-pleisztocén löszben előforduló
694 vulkáni képződménye Magyarországon: terepi és petrográfiai jellemzők (Middle
695 Pleistocene volcanic deposits in loess in Hungary: field and petrographical
696 characteristics). Földtani Közlöny 138, 297–310.
697 Schweitzer F, Szöőr G. 1997. Geomorphological and stratigraphical significance of Pliocene
698 red clay in Hungary. Zeitschrift für Geomorphologie, Supplement 110, 95–105.
699 Sheldon, N.D., Tabor, N.J., 2009. Quantitative paleoenvironmental and paleoclimatic
700 reconstruction using paleosols. Earth-Science Reviews 95, 1–52.

701 Shingvi, A.K., Bronger, A., Sauer, W., Pant, R.K., 1989. Thermoluminescence dating of
702 loess-paleosol sequences in the Carpathian Basin (East-Central Europe): a suggestion
703 for a revised chronology. Chemical Geology 73, 307–317.
704 Singer, B.S., Relle, M.K., Hoffman, K.A., Battle, A., Laj, C., Guillou, H., Carracedo, J.C.,
705 2002. Ar/Ar ages from transitionally magnetized lavas on La Palma, Canary Islands,
706 and the geomagnetic instability timescale. Journal of Geophysical Research 107 (B11),
707 2307. doi:10.1029/2001JB001613.
708 Stevens, T., Marković, S.B., Zech, M., Hambach, U., Sümegi, P., 2011. Dust deposition and
709 climate in the Carpathian basin over an independently dated last glacial–interglacial
710 cycle. Quaternary Science Reviews 30, 662–681.
711 Szebényi, E., 1979. Sedimentological and micromineralogical analysis of the southern profile
712 of the Paks loess exposure. Acta Geologica Hungarica 22, 427–432.
713 Taylor, S.R., McLennan, S.M., 1985. The Continental Crust: its Composition and Evolution.
714 Blackwell Scientific Publications Ltd., p. 312.
715 Tzedakis, P.C., Hooghiemstra, H., Pälike, H., 2006. The last 1.35 million years at Tenaghi
716 Philippon: revised chronostratigraphy and long-term vegetation trends. Quaternary
717 Science Reviews 25, 3416–3430.
718 Újvári, G., Varga, A., Balogh-Brunstad, Zs., 2008. Origin, weathering, and geochemical
719 composition of loess in southwestern Hungary. Quaternary Research 69, 421–437.
720 Újvári, G., Varga, A., Ramos, F.C., Németh, T., Stevens, T., in press. Evaluating the use of
721 clay mineralogy, Sr-Nd isotopes and zircon U-Pb ages in tracking dust provenance: an
722 example from loess of the Carpathian Basin. Chemical Geology.
723 Varga, A., Újvári, G., Raucsik, B., 2011. Tectonic versus climatic control on the evolution of
724 a loess–paleosol sequence at Beremend, Hungary: An integrated approach based on

paleoecological, clay mineralogical, and geochemical data. Quaternary International 240, 71–86.

Weaver, C.E., 1989. Clays, Muds, and Shales. Elsevier, Amsterdam.

Wintle, A.G., Packmann, S.C., 1988. Thermoluminescence ages for three sections in Hungary. Quaternary Science Reviews 7, 315–320.

Yang, S., Ding, F., Ding, Z., 2006. Pleistocene chemical weathering history of Asian arid and semi-arid regions recorded in loess deposits of China and Tajikistan. Geochimica et Cosmochimica Acta 70, 1695–1709.

Zanazzi, P.F., Montagnoli, M., Nazzareni, S., Comodi, P., 2007. Structural effects of pressure on monoclinic chlorite: A single-crystal study. American Mineralogist 92, 655–661.

Zhou, L.P., Shackleton, N.J., 1999. Misleading positions of geomagnetic reversal boundaries in Eurasian loess and implications for correlation between continental and marine sedimentary sequences. Earth and Planetary Science Letters 168, 117–130.

Zöller, L., Oches, E.A., McCoy, W.D., 1994. Towards a revised chronostratigraphy of loess in Austria with respect to key sections in the Czech Republic and in Hungary. Quaternary Geochronology (Quaternary Science Reviews) 13, 465–472.

Zöller, L., Wagner, G.A., 1990. Thermoluminescence dating of loess – recent developments. Quaternary International 7/8, 119–128.

Figures and captions

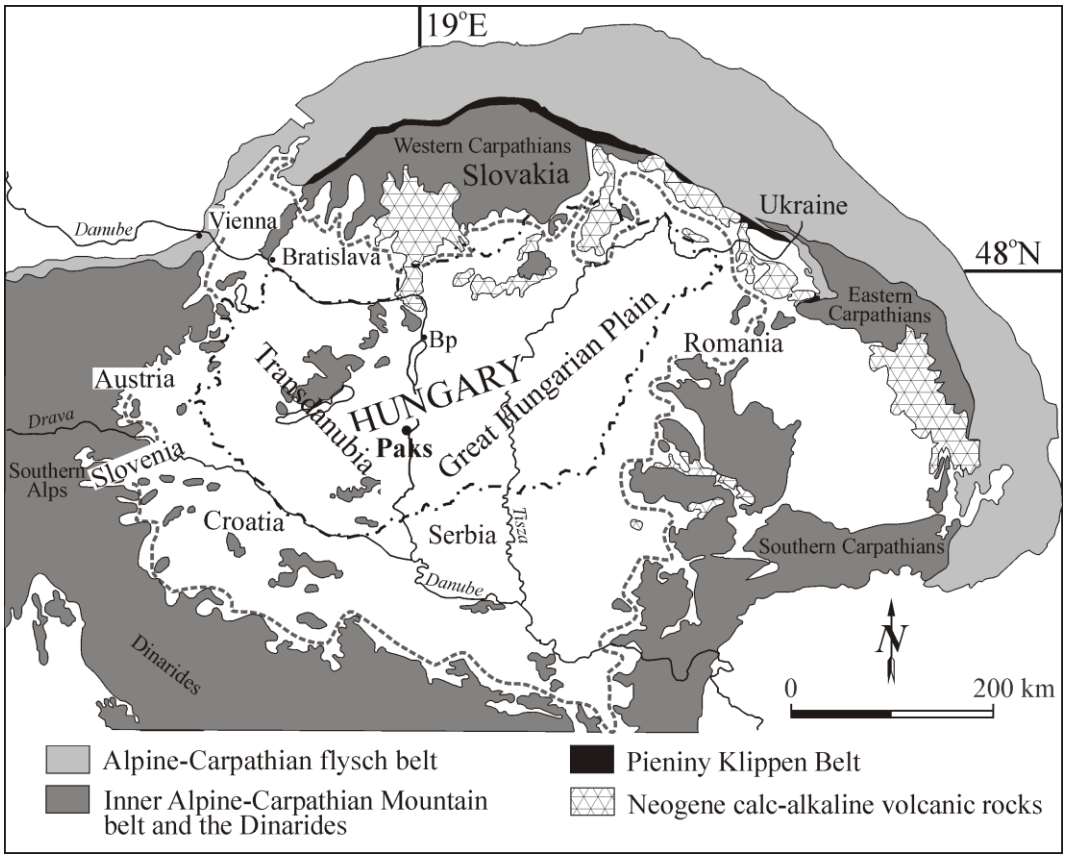

745

746 **Figure 1.** The Carpathian Basin with the location of sampling site at Paks (map is modified
747 from Varga et al., 2011). Gray, dashed line outlines the area of the Carpathian Basin, black
748 dot-dashed line indicates the border of Hungary.

749

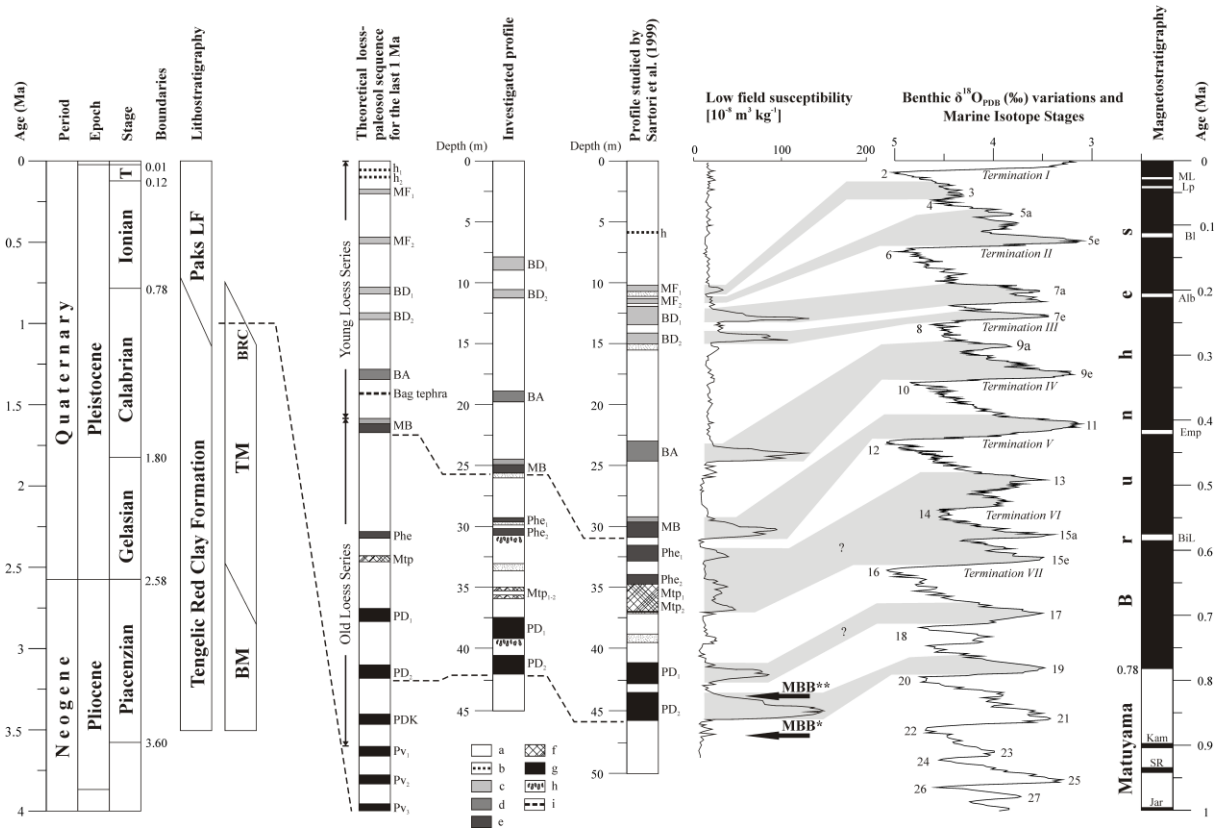

Figure 2. Geochronological and stratigraphic framework of the Hungarian red clays and loess-paleosol sequences with the stratigraphic position of the investigated profile at Paks. Global chronostratigraphy is from Gibbard and Cohen (2008). T= Tarantian, Paks LF= Paks Loess Formation, BM= Beremend Member, TM= Tengelic Member, BRC= Basal Red Clays of the Paks Loess Formation (after Pécsi, 1985; Jámbor, 1997; Schweitzer and Szöőr, 1997; Koloszár, 2004; Kovács et al., 2008, 2011). The theoretical loess-paleosol sequence and all related abbreviations are from Pécsi (1985, 1995, 1998): h_1= „Tápiósüly" humus horizon, h_2= „Dunaújváros" humus horizon, MF_1= Mende Upper 1 paleosol, MF_2= Mende Upper 2 paleosol; BD_1= Basaharc Double 1 fossil soil, BD_2= Basaharc Double 2 fossil soil, BA= Basaharc Lower paleosol, MB= Mende Base paleosol, Ph_1-Ph_2= Paks sandy soil complex, Mtp_{1-2}= hydromorphous soil at Paks, PD_1= Paks Double 1 paleosol, PD_2= Paks Double 2 paleosol, PDK= Paks-Dunakömlőd soil complex, Pv_1-Pv_3= basal red soils/red clays at Paks. MBB*= measured position of the Matuyama-Brunhes Boundary after Pécsi and Pevzner (1974) and Márton (1979). MBB**= measured position of the Matuyama-Brunhes

765 paleomagnetic reversal after Sartori et al. (1999) and Sartori (2000). Correlation of loess and
766 paleosol layers with the $\delta^{18}O$ record is after Gábris (2007), but slightly modified. Benthic
767 $\delta^{18}O$ curve is the LR04 Stack of Lisiecki and Raymo (2005) and the paleomagnetic record is
768 from Singer et al. (2002). Black corresponds to normal polarity. Abbreviations of the events:
769 ML= Mono Lake, Lp= Laschamp, Bl= Blake, Alb= Albuquerque, Emp= Emperor, BiL= Big
770 Lost, Kam= Kamikatsura, SR= Santa Rosa.
771 Legend (for theoretical columns and the studied profile): a= loess, b= A horizon – weakly
772 developed chernozem and syrosem, c= Ah horizon – degraded chernozem, d= AB horizon –
773 chernozem-brown forest soil, e= Bw horizon – brown forest soil, f= lessivé – pseudogley, g=
774 Bw horizon – brown forest soil (rubified), h= carbonate concretions, i= tephra layer. Soil
775 classification is after Bronger (2003).
776

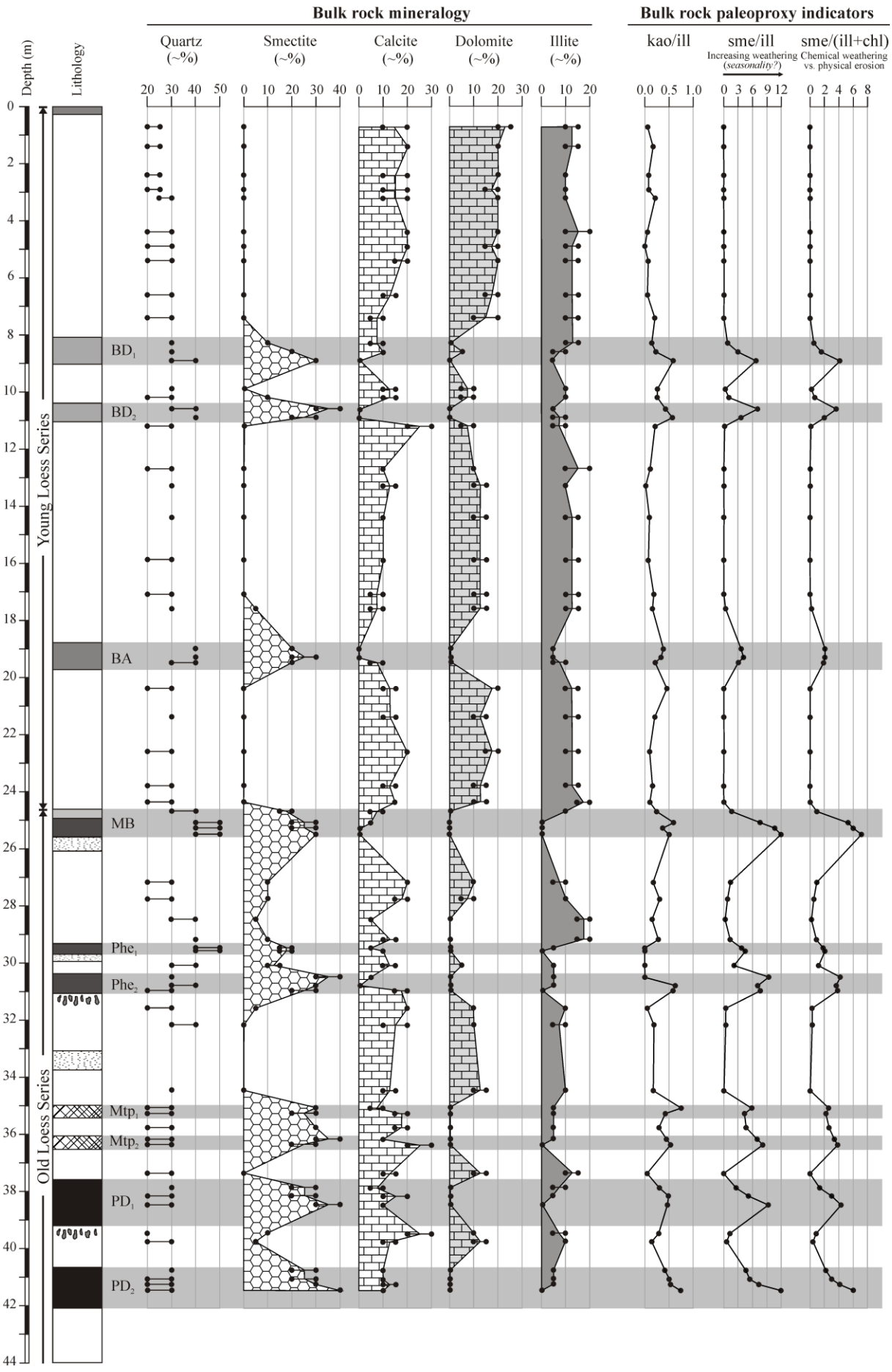
Bulk rock mineralogy
Bulk rock paleoproxy indicators
Depth (m)
Lithology
Quartz (~%)
Smectite (~%)
Calcite (~%)
Dolomite (~%)
Illite (~%)
kao/ill
sme/ill
Increasing weathering (seasonality?)
sme/(ill+chl)
Chemical weathering vs. physical erosion
Young Loess Series
Old Loess Series
BD1
BD2
BA
MB
Phe1
Phe2
Mtp1
Mtp2
PD1
PD2

778 **Figure 3.** Semi-quantitative bulk mineralogy (~%) of the loess and paleosol samples and
779 mineralogical proxy indicators of paleoenvironmental conditions, Paks section, Hungary.
780 Abbreviations: kao = kaolinite; ill = illite (±muscovite); sme = smectite; chl = chlorite.
781 Legend for lithology is the same as in Figure 2.

782

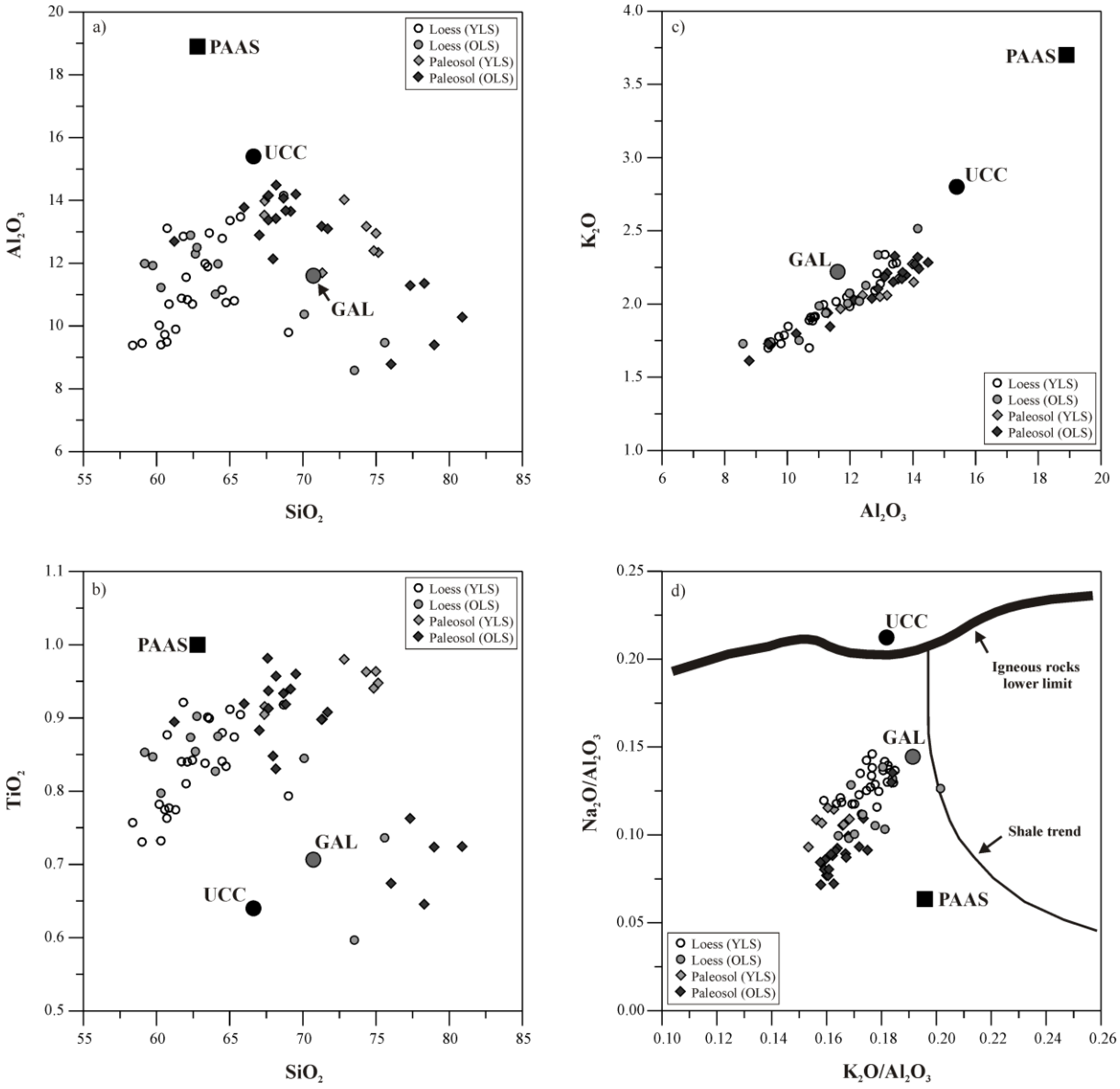

783

784 **Figure 4.** Diagrams of a) Al_2O_3 vs. SiO_2, b) TiO_2 vs. SiO_2, c) K_2O vs. Al_2O_3, and d)
785 Na_2O/Al_2O_3 vs. K_2O/Al_2O_3 for comparing the Paks YLS and OLS samples and average loess
786 composition (GAL, Global Average Loess; Újvári et al., 2008). Two standards, the post-
787 Archean Australian average shale (PAAS; Taylor and McLennan, 1985; McLennan, 2001)

788 and the Upper Continental Crust (UCC; Rudnick and Gao, 2003) are also shown. Loess and
789 paleosol samples plot in the sedimentary field under the igneous rocks lower limit (Garrels
790 and Mackenzie, 1971) and left from the shale trend (Gallet et al., 1998) in the Na_2O/Al_2O_3 vs.
791 K_2O/Al_2O_3 compositional space.
792

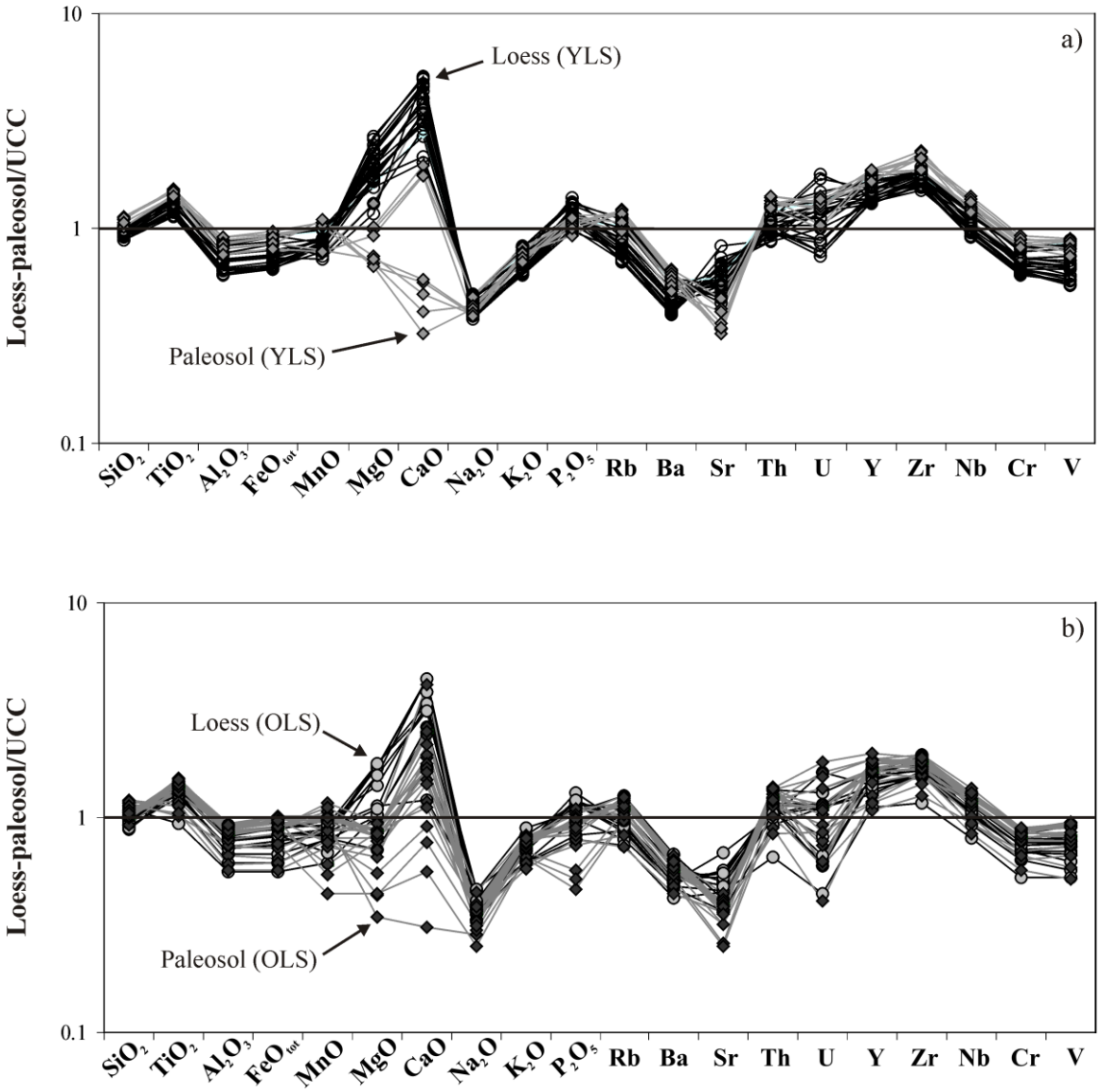

793

794 **Figure 5.** Major and trace element patterns normalized to UCC composition (Rudnick and
795 Gao, 2003) for (a) the YLS samples and (b) OLS samples.

796

797

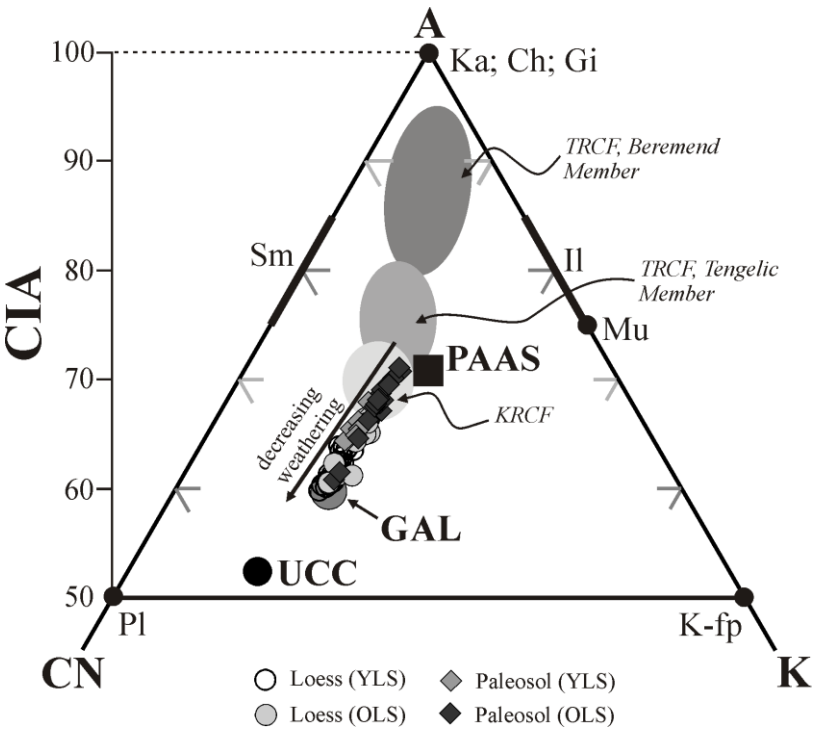

798

799 **Figure 6.** Ternary A–CN–K diagram (Nesbitt and Young, 1984) of the Paks loess and
800 paleosol samples (in molar proportions). The samples plot subparallel to the A–CN join,
801 suggesting an ideal weathering of a slightly more felsic source than the UCC (Rudnick and
802 Gao, 2003). Fields of the middle Pliocene to lower Pleistocene Tengelic Red Clay (TRCF)
803 and Kerecsend Red Clay (KRCF) samples (Kovács et al., 2011) are also shown for
804 comparison. Abbreviations are as follows: Sm = Smectite, Il = Illite, Mu = muscovite, Ka =
805 Kaolinite, Ch = Chlorite, Gi = Gibbsite, Pl = Plagioclase, K-fp = K-feldspar, and others as in
806 Fig. 4. Note that only the top 50% of the triangle is shown.

807

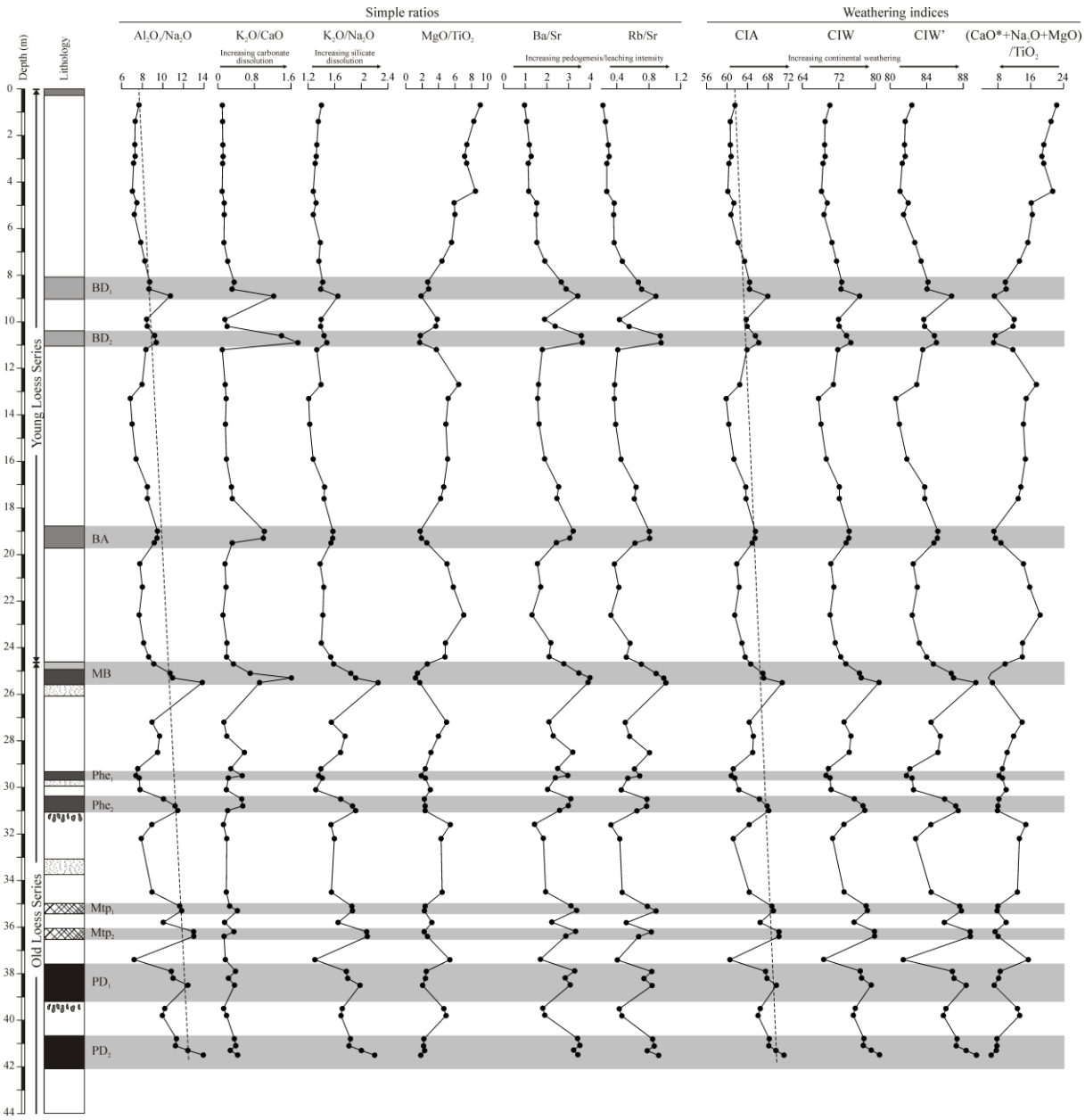

Figure 7. Bulk chemical proxy indicators of paleoenvironmental conditions, Paks section, Hungary. Abbreviations: CIA = Chemical Index of Alteration (Nesbitt and Young, 1982); CIW = Chemical Index of Weathering (Harnois, 1988); CIW' or CPA = modified Chemical Index of Weathering/Chemical Proxy of Alteration (Cullers, 2000; Buggle et al., 2011), $(CaO^*+Na_2O+MgO)/TiO_2$ (Yang et al., 2006). Legend for lithology is the same as in Figure 2.

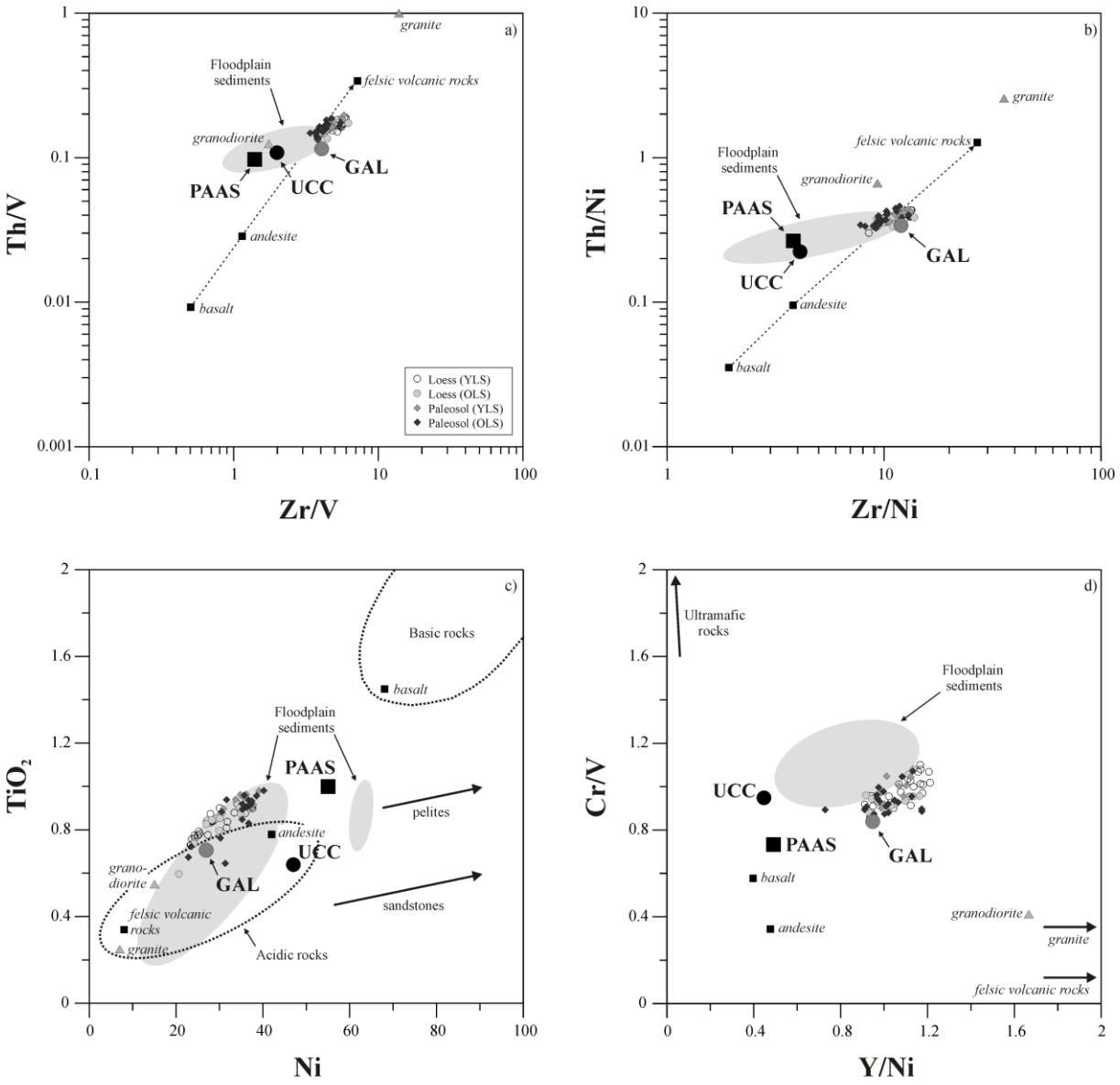

Figure 8. Plots of a) Zr/V vs. Th/V, b) Zr/Ni vs. Th/Ni, and provenance discrimination diagrams of c) Ni vs. TiO_2 (Floyd et al., 1989) and d) Y/Ni vs. Cr/V (Hiscott, 1984) for comparing loess and paleosol samples from the Paks section and global average loess composition (GAL; Újvári et al., 2008), post-Archean Australian average shale (PAAS; Taylor and McLennan, 1985; McLennan, 2001), and Upper Continental Crust (UCC; Rudnick and Gao, 2003). Geochemical data of Hungarian floodplain sediments are from the online database of FOREGS Geochemical Atlas of Europe (sample IDs: from N32E09F1 to N32E11F5) (Salminen et al., 2005). Igneous rock compositions on a) and b) are average

826 values from Condie (1993). In panel d) the samples were also compared to ultramafic rock
827 (UMF) and granite (GRN) compositions (Amorosi et al., 2002).
828

829

Table 1. Major (wt%) and trace element (ppm) composition of loess and paleosol samples from the Paks profile

Sample code	Pa-1	Pa-2	Pa-3	Pa-4	Pa-5	Pa-6	Pa-7	Pa-8	Pa-9	Pa-10	Pa-11	Pa-12	Pa-13	Pa-14
Depth (m)	0.70	1.40	2.40	2.90	3.20	4.40	4.90	5.40	6.60	7.40	8.30	8.60	8.90	9.90
Type	L	L	L	L	L	L	L	L	L	L	P	P	P	L
SiO_2	59.01	60.30	60.56	61.30	60.70	58.37	62.10	62.45	61.71	63.60	67.39	67.36	72.83	63.32
TiO_2	0.731	0.732	0.775	0.775	0.763	0.757	0.840	0.842	0.840	0.899	0.916	0.905	0.980	0.838
Al_2O_3	9.45	9.40	9.73	9.90	9.49	9.38	10.84	10.70	10.88	12.96	13.98	13.53	14.02	11.99
FeOtot	3.27	3.26	3.42	3.43	3.34	3.36	3.80	3.72	3.81	4.66	4.76	4.66	4.88	4.00
MnO	0.083	0.084	0.085	0.086	0.087	0.084	0.089	0.089	0.090	0.096	0.101	0.101	0.107	0.077
MgO	6.63	6.06	5.76	5.55	5.65	6.42	4.95	5.04	4.68	3.96	2.45	2.53	1.83	3.22
CaO	17.73	16.98	16.39	15.65	16.74	18.42	13.84	13.62	14.51	9.96	6.37	7.01	1.76	13.01
Na_2O	1.23	1.28	1.33	1.35	1.32	1.33	1.45	1.48	1.38	1.57	1.60	1.56	1.30	1.42
K_2O	1.72	1.74	1.78	1.79	1.73	1.70	1.91	1.89	1.91	2.14	2.27	2.17	2.15	1.98
P_2O_5	0.150	0.162	0.173	0.171	0.169	0.175	0.175	0.180	0.177	0.161	0.159	0.172	0.139	0.154
Total	100	100	100	100	100	100	100	100	100	100	100	100	100	100
LOI (%)	18.44	17.26	16.76	16.18	16.95	18.52	14.95	14.78	15.24	12.20	9.45	10.02	6.95	13.69
CIA	62	61	61	61	60	60	61	61	62	63	64	64	68	64
Sc	9	8	8	9	8	8	10	10	10	12	12	12	13	11
V	56	53	56	58	54	55	66	64	65	83	86	85	87	72
Cr	56	58	60	58	58	56	63	62	63	75	79	76	85	67
Ni	23	23	24	25	24	24	28	27	29	38	38	37	39	32
Cu	14	13	13	13	14	13	14	13	16	18	26	20	20	13
Zn	41	41	43	47	41	44	49	48	48	63	68	64	65	51
Ga	9	9	10	10	9	9	11	10	11	14	17	16	17	13
Rb	60	60	63	64	61	58	71	69	71	87	101	96	103	75
Sr	266	234	216	210	221	214	195	192	194	187	152	136	116	175
Y	28	27	29	29	28	29	32	32	31	36	38	37	39	31
Zr	306	310	324	327	320	298	344	347	337	338	361	359	415	326
Nb	11.0	11.1	11.8	11.8	11.5	10.9	13.0	12.7	12.6	14.2	15.2	14.8	16.9	13.0
Ba	258	251	256	267	252	248	298	289	298	355	403	392	398	330
La	31	30	33	33	30	32	37	37	37	38	45	39	43	36
Ce	59	62	67	68	63	61	71	65	68	79	87	83	95	70
Nd	25	29	30	30	25	28	31	30	30	35	37	37	39	32
Pb	12	11	12	13	13	13	14	14	14	17	18	17	20	15
Th	9	9	11	10	10	9	12	11	10	13	14	13	14	11
U	3	3	3	2	3	4	3	5	2	4	4	3	3	3

L: loess; P: paleosol; LOI: Loss on ignition; CIA: Chemical Index of Alteration (Nesbitt and Young, 1982).

Major elements are normalized on a volatile-free basis, with total Fe expressed as FeO.

830

831

832

Pa-21	Pa-22	Pa-23	Pa-24	Pa-25	Pa-26	Pa-27	Pa-28	Pa-29	Pa-30	Pa-31	Pa-32	Pa-33	Pa-34	Pa-35
14.40	15.90	17.10	17.60	19.00	19.30	19.50	20.40	21.40	22.60	23.80	24.40	24.70	25.10	25.30
L	L	L	L	P	P	P	L	L	L	L	L	P	P	P
65.31	63.49	65.01	65.73	75.15	74.84	71.33	64.75	64.48	60.18	61.83	60.72	68.15	77.33	80.89
0.874	0.901	0.912	0.905	0.948	0.941	0.898	0.834	0.841	0.782	0.921	0.877	0.831	0.763	0.724
10.80	11.89	13.36	13.48	12.34	12.40	11.69	10.75	11.15	10.02	12.85	13.11	13.42	11.29	10.28
3.67	4.24	4.69	4.64	4.27	4.33	4.02	3.66	3.78	3.49	4.62	4.66	4.54	3.63	3.24
0.084	0.090	0.085	0.099	0.110	0.079	0.077	0.083	0.083	0.083	0.100	0.099	0.100	0.088	0.095
4.27	4.59	4.21	3.84	1.66	1.80	2.30	4.18	4.87	5.52	4.45	4.19	2.18	1.08	0.85
11.38	10.94	7.68	7.24	2.01	2.07	6.28	12.27	11.24	16.60	11.24	12.31	6.85	2.74	1.12
1.54	1.61	1.57	1.58	1.30	1.31	1.27	1.38	1.39	1.30	1.58	1.52	1.47	1.05	0.94
1.89	2.05	2.27	2.28	2.05	2.06	1.97	1.91	2.00	1.85	2.21	2.34	2.33	1.94	1.80
0.186	0.209	0.198	0.195	0.170	0.171	0.167	0.176	0.176	0.173	0.193	0.171	0.137	0.085	0.070
100	100	100	100	100	100	100	100	100	100	100	100	100	100	100
12.73	12.79	10.70	10.40	5.48	5.83	8.81	13.28	13.18	16.48	13.16	13.56	9.10	5.83	4.31
60	61	64	64	66	65	65	62	62	61	63	64	65	67	67
10	11	11	12	11	11	12	10	9	9	12	12	13	9	9
64	72	81	86	78	75	72	63	67	59	82	80	83	71	65
65	66	75	74	79	79	75	65	67	63	74	74	74	65	59
28	30	35	37	36	34	31	28	28	25	34	36	37	30	27
14	18	21	23	20	19	16	12	13	12	19	19	19	14	11
48	55	64	67	58	59	53	46	50	43	62	64	65	51	46
10	13	15	14	13	14	13	11	12	9	14	14	15	12	12
71	77	92	93	89	90	82	67	75	65	87	90	101	91	82
184	170	144	151	110	111	131	182	177	200	154	173	142	102	83
30	34	37	35	39	34	35	31	32	29	36	33	33	31	25
364	348	348	350	440	435	411	371	373	332	334	306	301	310	307
12.7	14.2	14.5	15.0	15.7	15.8	14.2	12.3	12.5	12.0	14.1	13.6	14.2	13.2	12.1
301	322	366	370	354	339	319	284	303	263	336	364	395	353	331
37	39	43	39	45	41	39	33	35	32	41	35	40	32	32
69	76	88	83	83	86	78	71	68	62	82	79	76	67	65
31	33	37	36	38	35	33	31	32	29	37	35	32	30	25
13	16	18	18	18	17	16	15	15	13	16	17	20	18	18
12	11	13	13	15	15	13	12	11	10	12	11	12	13	12
5	3	4	4	4	4	4	3	3	2	3	4	3	2	3

833
834

835

Pa-42	Pa-43	Pa-44	Pa-45	Pa-46	Pa-47	Pa-48	Pa-49	Pa-50	Pa-51	Pa-52	Pa-53	Pa-54	Pa-55	Pa-56
29.60	30.10	30.50	30.80	31.00	31.60	32.20	34.50	35.10	35.30	35.80	36.20	36.40	37.40	37.90
P	L	P	P	P	L	L	L	P	P	L	P	P	L	P
76.02	70.09	71.27	71.68	67.96	60.30	73.52	64.19	65.98	68.16	62.65	67.58	61.21	64.02	67.65
0.674	0.845	0.898	0.908	0.848	0.797	0.597	0.875	0.920	0.957	0.854	0.982	0.895	0.827	0.937
8.78	10.37	13.17	13.10	12.13	11.22	8.58	11.98	13.78	14.49	12.30	14.13	12.69	11.01	14.15
2.88	3.38	4.62	4.56	4.24	3.91	2.83	4.10	4.94	5.12	4.19	5.09	4.53	3.75	5.05
0.074	0.079	0.106	0.098	0.080	0.082	0.062	0.084	0.097	0.086	0.086	0.101	0.117	0.086	0.086
1.61	2.53	2.03	2.14	2.00	4.32	2.57	3.88	2.17	2.17	2.72	2.20	2.36	4.44	2.34
7.09	9.47	4.23	4.02	9.49	15.99	8.92	11.30	8.57	5.36	13.80	6.44	15.04	12.18	6.01
1.14	1.33	1.31	1.17	1.06	1.26	1.08	1.34	1.18	1.22	1.22	1.09	0.98	1.53	1.31
1.61	1.75	2.21	2.19	2.03	1.94	1.73	2.07	2.20	2.28	2.02	2.26	2.04	1.99	2.32
0.118	0.148	0.142	0.142	0.164	0.173	0.119	0.181	0.164	0.155	0.166	0.125	0.150	0.174	0.140
100	100	100	100	100	100	100	100	100	100	100	100	100	100	100
7.95	10.54	8.12	8.03	11.34	16.04	9.90	13.06	9.25	11.22	13.94	10.12	15.08	13.21	9.48
62	62	66	68	68	64	61	64	69	69	66	70	70	61	68
8	10	12	11	11	9	8	11	12	14	12	14	11	11	13
50	61	81	79	75	68	51	74	89	93	73	89	76	66	89
53	65	79	79	73	64	49	70	78	81	68	83	72	63	81
23	27	36	36	35	30	21	30	37	39	30	40	35	27	37
12	13	23	20	18	17	10	19	22	23	16	23	20	16	20
41	44	68	65	60	54	38	58	66	71	55	71	59	50	70
9	11	15	15	13	12	10	12	16	17	12	16	12	11	17
62	67	98	98	86	71	63	79	98	106	80	103	86	74	103
115	147	127	127	132	219	144	169	125	120	154	124	128	182	123
25	31	35	36	34	28	23	34	36	39	33	39	34	31	37
276	376	342	353	325	297	226	351	334	354	320	378	328	341	347
10.1	12.1	14.7	15.1	13.8	12.5	9.6	13.9	15.2	15.4	13.1	16.5	14.3	12.8	15.5
275	299	392	379	341	313	264	329	389	403	343	413	368	309	403
29	35	41	43	38	29	26	36	39	44	33	45	39	32	39
51	70	84	84	72	68	50	72	80	89	67	89	76	71	82
22	32	36	36	32	30	23	33	35	39	30	37	36	31	36
12	15	19	19	17	13	13	15	18	20	15	20	17	14	18
9	11	13	14	12	11	7	12	13	13	12	14	13	12	15
2	2	4	3	3	3	1	3	2	4	2	4	4	2	2

836
837

838

Pa-63	Pa-64
41.30	41.50
P	P
67.64	69.52
0.913	0.960
13.37	14.20
4.57	4.92
0.112	0.076
2.10	1.76
7.92	5.18
1.08	1.02
2.15	2.24
0.147	0.135
100	100
10.87	9.29
70	71
12	12
83	92
78	82
37	36
21	23
62	68
13	16
96	105
123	114
39	42
349	368
15.1	15.6
397	390
42	42
77	87
37	39
17	20
13	14
2	5

839

840